ELSEVIER

Sheet flow and suspended sediment due to wave groups in a large wave flume

C. Marjolein Dohmen-Janssen[a,*], Daniel M. Hanes[b,c]

[a]*Department of Civil Engineering, University of Twente, Water Engineering and Management, P.O. Box 217, 7500 AE Enschede, The Netherlands*
[b]*Coastal and Marine Geology Program, US Geological Survey, 400 Natural Bridges Drive, Santa Cruz, CA 95060, USA*
[c]*Civil and Coastal Engineering, University of Florida, Gainesville, USA*

Abstract

A series of sand bed experiments was carried out in the Large Wave Flume in Hannover, Germany as a component of the SISTEX99 experiment. The experiments focussed on the dynamic sediment response due to wave group forcing over a flat sand bed in order to improve understanding of cross-shore sediment transport mechanisms and determine sediment concentrations, fluxes and net transport rates under these conditions. Sediment concentrations were measured within the sheet flow layer (thickness in the order of 10 grain diameters) and in the suspension region (thickness in the order of centimetres). Within the sheet flow layer, the concentrations are highly coherent with the instantaneous near-bed velocities due to each wave within the wave group. However, in the suspension layer concentrations respond much more slowly to changes in near-bed velocity. At several centimetres above the bed, the suspended sediment concentrations vary on the time scale of the wave group, with a time delay relative to the peak wave within the wave group. The thickness of the sheet flow changes with time. It is strongly coherent with the wave forcing, and is not influenced by the history or sequence of the waves within the group. The velocity of the sediment was also measured within the sheet flow layer some of the time (during the larger wave crests of the group), and the velocity of the fluid was measured at several cm above the sheet flow layer. The grain velocity and concentration estimates can be combined to estimate the sediment flux. The estimates were found to be consistent with previous measurements under monochromatic waves. Under these conditions, without any significant mean current, the sediment flux within the sheet flow layer was found to greatly exceed the sediment flux in the suspension layer. As a result, net transport rates under wave groups are similar to those under monochromatic waves.
© 2004 Elsevier Ltd. All rights reserved.

Keywords: Wave flume experiments; Wave groups; Sediment transport; Sheet flow; Suspension; Time-lag

*Corresponding author. Tel.: +31 53 48 4209; fax: +31 53 489 5377.
E-mail addresses: c.m.dohmen-janssen@ctw.utwente.nl (C.M. Dohmen-Janssen), dhanes@usgs.gov (D.M. Hanes).

1. Introduction

Nearshore morphology is determined by small-scale near-bed sediment transport processes. This is especially true under sheet flow conditions, when ripples are washed out and sand is transported close to the bed in a very thin layer with a thickness in the order of 10 grain diameters. Sheet flow transport is important for cross-shore morphology, because it corresponds to the high-energy flat bed regime that results in large quantities of transported material. Sediment transport in oscillatory sheet flow has often been studied in oscillating water tunnels (e.g. King, 1991; Dibajnia and Watanabe, 1992; Ribberink and Al-Salem, 1994, 1995; Dohmen-Janssen et al., 2001, 2002). To investigate whether these results are representative for the field situation experiments on near-bed processes were performed under prototype surface waves in the large wave flume of the ForschungsZentrum Küste (FZK) in Hannover, Germany (SISTEX99: Small-scale International Sediment Transport Experiments 1999). The experiments were the first in which both sand concentrations and grain velocities inside the sheet flow layer were measured under waves (see Ribberink et al. (2000) for an overview of these experiments). Time-dependent profiles of suspended sediment concentration above the sheet flow layer were also measured. Dohmen-Janssen and Hanes (2002) presented results from experiments in which sheet flow conditions were forced with monochromatic waves. They showed that there are strong similarities between the results from oscillating water tunnels and those from surface gravity waves.

This paper focuses on experiments on repetitive wave groups with large wave heights over a flat bed (sheet flow conditions). In the past, field observations showed that suspension events are strongly related to wave groups. Typically, sediment is entrained from the bed during the first few waves in the group, followed by "pumping up" of sediment to progressively greater heights during later waves (e.g. Hanes, 1991; Hay and Bowen, 1994; Vincent and Hanes, 2002). This phenomenon would not be expected in the sheet flow layer, which is located so close to the bed that sediment is expected to react almost instantaneously to the local hydrodynamic conditions. Data on sediment concentrations in the sheet flow and suspension layers are used to investigate whether the presence of wave groups affects the concentration behaviour in the sheet flow layer and to analyse "pumping up" processes in the suspension layer. In addition, suspended fluxes and sediment fluxes in the sheet flow layer (derived from measured concentrations and grain velocities) are analysed to calculate the contribution of the suspended load and the sheet flow to the total transport rate.

2. Experimental set-up

The large wave flume of the University of Hannover has a total length of 300 m, a width of 5 m and a depth of 7 m, with a wave paddle at one end and a 1:6 sloping dike at the other end. Measurements were carried out in the middle of a 75 cm thick, 45 m long horizontal sand bed in the central part of the flume, consisting of well-sorted sand with a median grain size of 0.24 mm. A 1:10 sloping beach consisting of somewhat coarser sand
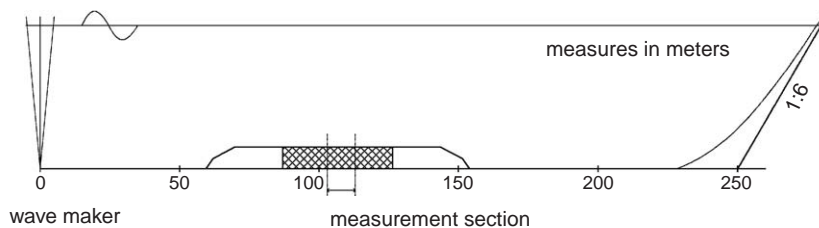

Fig. 1. Outline of the wave flume with the test section. The wave paddle is on the left side and the beach is on the right side. Distance is in meters, with a vertical exaggeration of approximately 8:1.

($D_{50} = 0.3$ mm) was placed against the 1:6 dike in order to dissipate the wave energy (Fig. 1).

Sediment concentrations and grain velocities at different elevations inside the sheet flow layer were measured using a conductivity concentration meter system (CCM, developed by Delft Hydraulics) that was specifically developed for the current flume tests. The system consists of two probes installed in a waterproof enclosure that was buried under the sand bed, such that the CCM-probes penetrated the sheet flow layer from below. The sensor could be moved up and down using a remotely controlled vertical positioning system (Dohmen-Janssen and Hanes, 2002). The CCM is designed to measure high sand concentrations (≈ 100–2000 g/l or 0.04–0.75 by volume). It measures the electro-conductivity of the sand-water mixture, which is related to the volume concentration of sand. The height of the sensing volume is approximately 1–1.5 mm (for more details about the CCM-probes and their measuring volumes, see Ribberink and Al-Salem, 1995). In the current experiments, two CCM probes were used at the same vertical elevation but separated by 15 mm in the horizontal flow direction in order to determine grain velocities by cross-correlation of the two concentration signals. This technique is based on the assumption that the time lag between correlated fluctuations in concentration reflects the time of flight of the grains between the two sensing volumes (that is, at the top of the CCM-sensors and thus inside the sheet flow layer).

Time-varying suspended sediment concentration profiles were measured using several Acoustic Backscatter Sensors (ABS, as described by Thorne and Hanes, 2002). Near-bed flow velocities (outside the wave boundary layer) were measured using three acoustic Doppler velocimeters (ADV). One ADV was positioned with its measurement volume at about 0.1 m above the bed near the location of the CCM (at the same along-tank position, 35 cm offset in across-tank direction) and two ADVs were positioned near the location of the ABSs, at about 0.08 and 0.14 m above the bed. The ABS and the CCM were offset by approximately 1 m in the cross-tank direction and 3 m in the along-tank direction. The ADV near the CCM was also used to measure the height of the sand bed during a run.

Experimental conditions presented in this paper consisted of repetitive 'natural' wave groups. The wave groups were generated by selecting one wave group from a narrow-banded Jonswap spectrum ($\gamma = 10$) and repeating this wave group about 20 times in each experimental run. In this paper, we focus on one series of the flat bed sheet flow conditions called Gp. During this series of experiments the wave group period, T_{gr}, was 90 s. The peak wave period, T_p, was 9.1 s, and the design significant wave height at the wave paddle, H_s, was 0.9 m. The water depth at the wave paddle was 3.75 m, corresponding to a water depth above the sand bed of 3.0 m. The appearance of the wave group can be seen in Fig. 2, which shows the water surface elevation during the passage of two wave groups. This figure also shows that waves were clearly asymmetric, reflecting shallow water conditions.

The seabed was almost flat under these wave conditions. Fig. 3 shows the seabed profile over three different length scales: (a) the entire test section, (b) a 2.5 m section, and (c) a 0.5 m section. The figure shows that some large-scale bed patterns are present. However, the slope of these bed
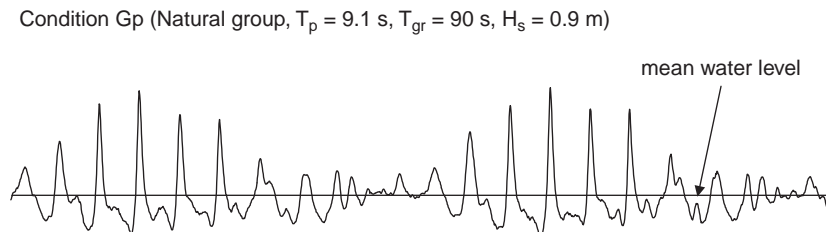
Condition Gp (Natural group, T_p = 9.1 s, T_{gr} = 90 s, H_s = 0.9 m)

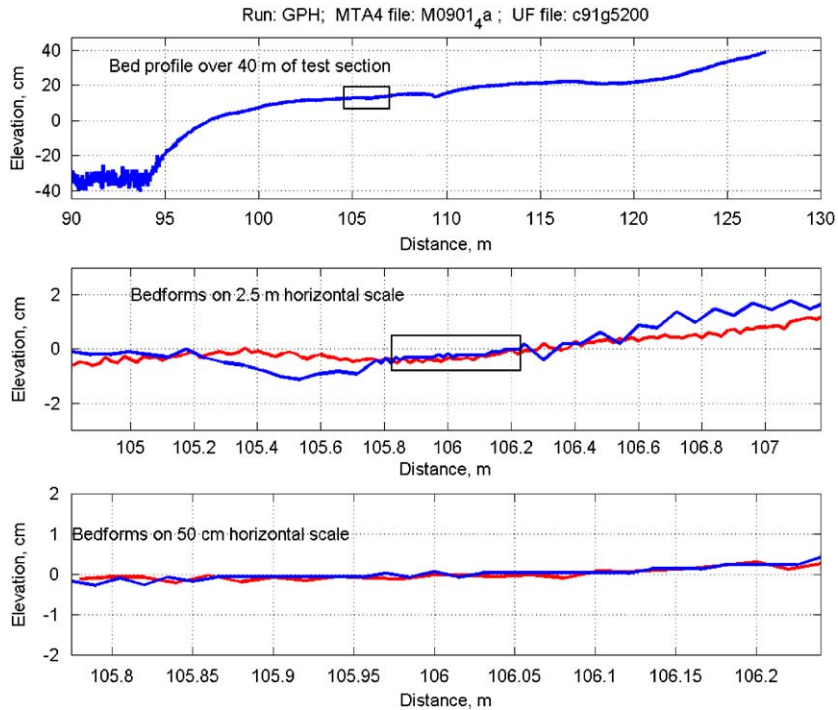Fig. 2. Water level elevation during passage of two wave groups of condition Gp.

Fig. 3. Seabed profile during run Gp. The two lines in the bottom two panels indicate the beginning (blue) and end (red) of the 30 min experimental run.

features is minimal (generally less than 0.01) and the bed can reasonably be considered to be flat.

3. Results and discussion

3.1. Time-averaged concentrations

Fig. 4 shows the concentration profile in the sheet flow layer after time averaging over the wave group. All measured concentrations are grouped in bins, based on their average value during the wave group. The average bin-concentrations are plotted against the average bin-levels (open circles in the figure), together with their standard deviations. The level $z = 0$ is defined as the level of the initial still bed. Because the sheet flow is very thin and exhibits large concentration gradients, it is important to determine the still bed level with greater accuracy than is typically achieved in laboratory experiments. We utilize the concentration measurements to determine the location of the still bed
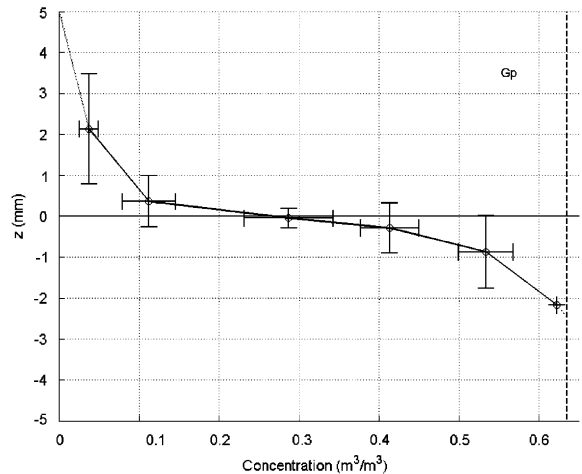

Fig. 4. Time-averaged concentration profile for test condition Gp.

level such that the amount of sand that is 'missing' below $z = 0$ during the experiment is equal to the amount of moving sand, that is, the total load. The

details of this technique are as follows: The measured time-averaged concentration profile in the sheet flow layer is extrapolated to its boundaries (thin dashed lines in Fig. 4). The right-hand-side of the concentration profile is extrapolated to the still bed value, which is the maximum concentration during the wave group at the lowest measuring point. The still bed concentration is indicated in Fig. 4 by the vertical dashed line. At the left-hand-side of Fig. 4, the concentration profile is extrapolated to the height of the lowest measured point in the suspension layer, which indicates a time-averaged concentration of the order of 10^{-4} m^3/m^3 at approximately 5 mm above the bed. The area below $z = 0$, above the concentration profile and to the left of the vertical dashed line, represents the amount of sand 'missing' from the bed. By conservation of mass this area is should be equal to the integration of the concentration profile above $z = 0$, that is, the total load. In this case, the still bed level had to be shifted down 0.27 mm compared to the original estimates of the elevation of the measuring points. The original estimates were based on measurements of the elevation of the CCM-probe relative to the concrete bottom and measurements of the height of the sand bed above the concrete bottom, recorded by the ADV that was closest to the CCM.

Fig. 4 shows clearly that a sharp vertical concentration gradient is present close to the bed: time-averaged concentrations decrease from 0.63 m^3/m^3 at approximately 2.5 mm below the initial bed level to a value of about 0.04 m^3/m^3 at approximately 2 mm above the initial bed level. The concentrations in the suspension layer above the sheet flow are two to three orders of magnitude smaller than in the sheet flow layer, and the gradient of the concentration is also significantly smaller in the suspension layer. Fig. 5 shows the time-averaged sediment concentration measured by the acoustic backscatter sensors, a pump sampler, and the CCM. The vertical locations of the various measurement points have been very slightly shifted in the following ways in order to provide good visualization on a log-scale: to display the CCM data using a log scale in Fig. 5, the CCM elevations have been shifted vertically such that the lowest measurement, which is
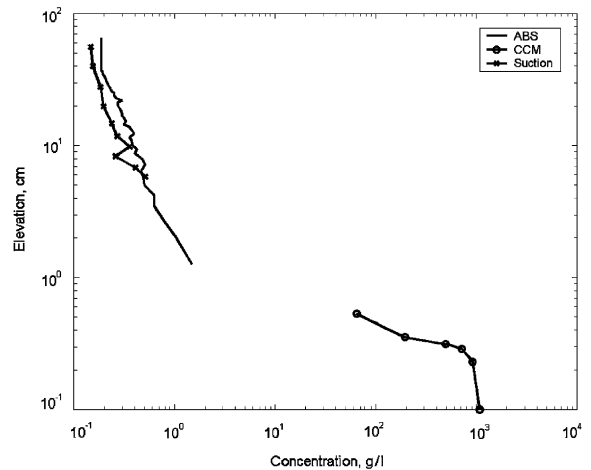

Fig. 5. Time-averaged concentration profile for the ABS, pump samples, and CCM data.

actually located 2.2 mm below the still bed level, is displayed in Fig. 5 at an elevation of 1 mm (all measurement points are shifted up 3.2 mm). The vertical location of the ABS has a large uncertainty (about 10 mm), compared to the vertical resolution of the CCM measurements. The lowest data point is estimated to be about 6–14 mm above the still bed, that is, on average about 10 mm above the still bed. Shifting the ABS elevations over the same distance as the CCM elevations yields a lowest elevation of ABS measurements of about 13 mm above the bed. The lowest data point of the suction sampler is located between 55 and 74 mm above the still bed and is estimated to be at 56 mm above the still bed. Shifting these levels also over the same distance yields an elevation of the lowest data point of the suction sampler of about 5.9 cm above the still bed. We note that these small shifts are merely to aid visualization on a log-scale, since some of the CCM measurements are actually at negative elevations.

No net current is present in the wave flume, apart from the return flow, which is small in this region where waves are not breaking yet; ADV measurements indicate return flow velocities of a about 0.02 m/s at an elevation of about 0.1 m above the bed. In field conditions, where net currents with larger magnitudes are usually present, higher suspended sediment concentration and

higher net suspended flux are expected. The small net current velocities in the wave flume correspond to small current friction velocities u_{fc}. This means that above the wave boundary layer the suspension parameter w_s/u_{fc} is much larger than 1, indicating that suspension above the wave boundary layer is indeed negligible in this case.

3.2. Time-dependent sediment concentrations during the wave group

Fig. 6 shows the temporal variations of the ensemble-averaged flow velocities and sediment concentrations. The upper panel presents the concentrations at different levels inside the sheet flow layer, that is, just below and above the initial bed level ($z = 0$). The numbers to the right of the figure give the elevations with respect to the initial bed level (in mm). The measurements are ensemble-averaged over several wave groups. The numbers between parentheses present the number of wave groups over which the ensemble-average is determined. This number varies because the sensor is moved vertically—but not uniformly—over the course of the experiment in order to obtain

measurements at different elevations within the sheet flow layer. The middle panel shows the ensemble-averaged suspended sediment concentrations at two different elevations. The lowest obtainable measurement of suspended sediment concentration, which is approximately 6–14 mm above the bed, is shown as well as the concentration 74 mm above the bed. The lower panel presents the measured flow velocity just outside the wave boundary layer (at $z = 0.1$ m). Near-bed velocities are very asymmetric, with maximum crest velocities of about 1.5 m/s and maximum trough velocities of about 0.8 m/s. This asymmetric behaviour is clearly reflected in the sediment concentrations.

From the concentration measurements in the sheet flow layer, two different layers can be identified: a pick-up layer located below the initial bed level (that is, $z < 0$) and an upper sheet flow layer located above the initial bed level (that is, $z > 0$). This two-layer system is very similar to what was observed in the past in oscillating water tunnels (for example, Ribberink and Al-Salem, 1995; Dohmen-Janssen et al., 2002) and under monochromatic waves (Dohmen-Janssen and Hanes, 2002).
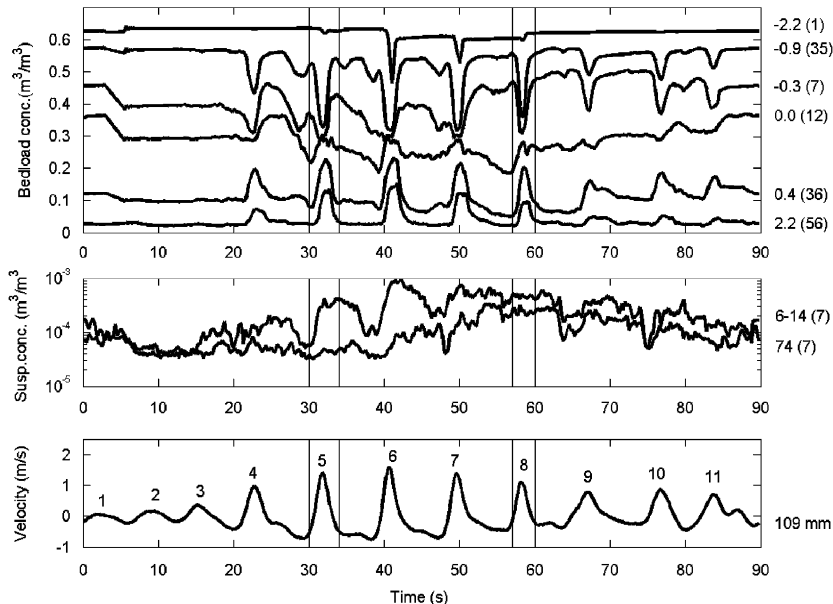

Fig. 6. Ensemble-averaged concentrations in the sheet flow layer (upper panel) in the suspension layer (middle panel), together with ensemble-averaged near-bed velocities outside the wave boundary layer (at 0.1 m above the bed, lower panel).

At the lowest elevation ($z = -2.2$ mm), the concentration during most of the wave group is equal to the concentration of the sand bed. Sediment is picked up from the bed only under the crest of the largest waves (largest near-bed velocities), resulting in a decrease in concentration at the moment of maximum (crest) velocity. At a slightly higher elevation ($z = -0.9$ mm), sediment is also picked up under the crest of smaller waves and under the trough of the high waves. The decrease in concentration is strongest under the largest wave and the decrease in concentration under the crest of the wave is much stronger than under the trough of the wave. This indicates that the concentration in the pick-up layer is directly and nearly simultaneously related to the near-bed hydrodynamics. In other words, the time-lag between the velocity and the concentration is very small.

Above the initial bed, in the upper sheet flow layer ($z = +0.4$ mm; $z = +2.1$ mm), concentrations increase when the near-bed velocity increases; grains that are picked up from below the still bed level are entrained into the flow just above the still bed level. Again, the peak in concentration is largest under the crest of the largest wave. Decreasing velocities under the following smaller waves lead to lower concentration peaks. The concentration peaks under the wave troughs are much smaller than under the wave crests, as a result of the much smaller trough velocities and shear stresses compared to under the crest. Thus, the sediment concentrations in the upper sheet flow layer also appear to be highly coherent with the near-bed hydrodynamics.

The suspended sediment concentrations indicate a temporal response quite different from the bedload sheet flow, particularly at higher elevations above the bed and as the waves occur later in the group. Close to the bed there is an increase in suspended sediment concentration that corresponds to the increasing velocity under the crest of each of waves 3–7. There is also a decrease in concentration during each subsequent wave trough, but this decrease occurs over a longer time scale than the response of the bedload concentrations. Further into the wave group, the response to the individual waves becomes progressively weaker, with the suspended sediment con-

centration remaining elevated during the small waves at the end of the wave group. Higher above the bed, the slow time response of the suspended sediment is more obvious. Here the response to individual waves is small and the concentration increases and then decreases over the time scale of the wave group, with a time delay relative to the peak wave within the wave group. This is generally referred to as the 'pumping up' process. The 'pumping up' process observed in the present flume tests in the suspension layer is described in greater detail by Vincent and Hanes (2002).

Although the concentrations in the suspension layer depend on the sequence of waves in the wave group, concentrations closer to the bed (that is, in the sheet flow layer) depend on the phase in each individual wave. Recent simulations by Hsu and Hanes (2004) indicated that for coarse sand a phase lag may occur between fluid velocities and sediment concentrations in the bed load layer. They found that concentrations are related to acceleration as well as the free-stream velocity. The fact that we hardly see any phase lag between velocity and concentrations might be explained by the fact that for these highly nonlinear waves, the peak in acceleration occurs at nearly the same time as the peak in velocity, as can be seen in Fig. 7. This figure shows the velocity in the upper panel and the acceleration in the lower panel. The vertical lines indicate the times in the wave group when the near-bed velocity under the highest waves is at its maximum. These are very close to the times of maximum acceleration and deceleration.

The direct relation between the near-bed velocity and the concentration inside the sheet flow layer is illustrated in a slightly alternate manner in Fig. 8, which shows the crest velocity of the different waves in the group as a function of wave sequence, and the corresponding instantaneous values of the concentration at the times of peak near-bed velocities at the various elevations inside the sheet flow layer. This figure shows that the concentrations inside the sheet flow layer follow the near-bed velocities: the highest concentration in the upper sheet flow layer and the strongest decrease in concentration in the pick-up layer occur under the highest wave (that is wave 6;
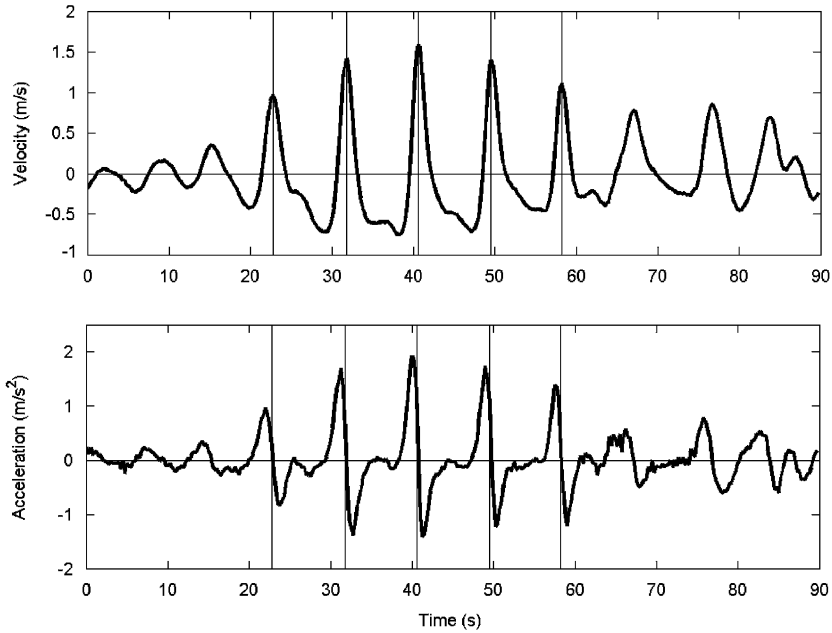
Fig. 7. Ensemble-averaged fluid velocities (upper panel) and fluid accelerations (lower panel) at 0.1 m above the bed.
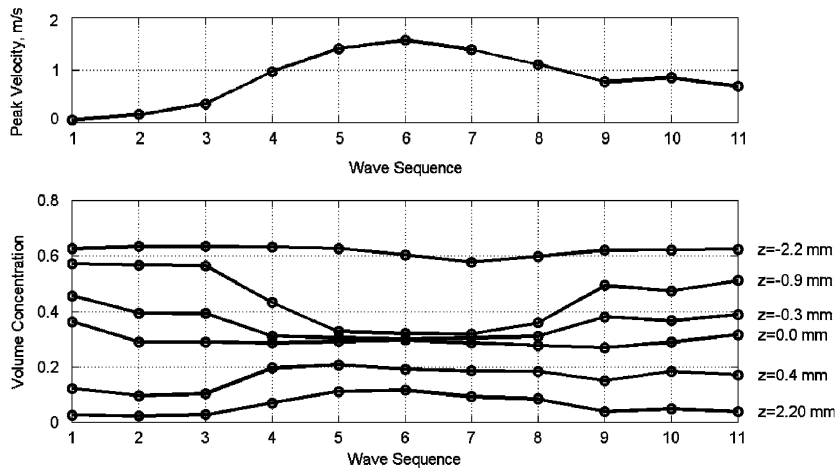

Fig. 8. Concentrations at different elevations inside the sheet flow layer under the wave crest, in relation to the near-bed velocity, for different consecutive waves in the wave group.

highest crest velocity). When the waves decrease again (waves 7, 8 and 9) concentrations in the upper sheet flow layer decrease again and similarly, concentrations in the pick-up layer increase again. Again, no time history effects over the time scale of a wave group appear in the sheet flow layer.

3.3. Vertical concentration profile and sheet flow layer thickness

Fig. 9 shows the vertical profile of sediment concentration in the sheet flow layer under the crest and trough of the highest wave in the group (wave 6). Again, the level $z = 0$ is determined by

shifting this level until the amount of sand that is 'missing' below $z = 0$, is equal to the total load. To achieve this, the levels had to be shifted down 0.05 and 0.32 mm for the concentration profile under the trough and the crest of the wave, respectively. The fact that the shift in level under the trough of the wave is different than that under the crest of the wave indicates that there is some uncertainty about the exact elevation of each measurement point. However, the difference is rather small (0.27 mm) and is well within the approximate height of the sensing volume (vertical resolution) of the CCM (1–1.5 mm). The dotted lines indicate the estimated extrapolation of the concentration profile beyond the measurement points.

Under the trough of the wave, the concentration at 2.1 mm below the initial bed is almost equal to the still bed concentration. Above this level, the concentration shows a very sharp vertical gradient going from a volume concentration of 0.6–0.1 over less than 3 mm. Under the crest, more sediment is picked up due to the larger near-bed velocity and the concentration at the lowest elevation ($z = -2.1$ mm) is smaller than the still bed concentration. The concentration gradient under the crest of the wave is smaller than under the trough of the wave.
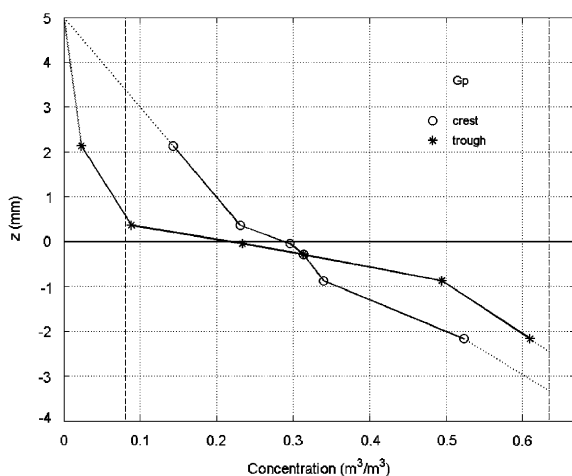
In general, the sheet flow layer is defined as the layer where concentrations are so high that intergranular forces are important. Therefore, following Bagnold (1956), the top of the sheet flow layer is defined as the level where the concentration reaches a value of about 0.08. This is the concentration for which the distance between hexagonally packed spheres, is on average, equal to their diameter. It can be expected that for higher concentrations intergranular forces become important. It is reasonable to assume that the bottom of the (mobile) sheet flow layer is located at the level where the sediment concentration reaches the value of the still bed concentration ($c \approx 0.63$).

These two limiting concentration values are indicated in Fig. 9 by the vertical dashed lines. They can be used to estimate the thickness of the sheet flow layer under the crest and under the trough of the wave. For example, for the concentration profiles presented in Fig. 9 this yields the following results. At the time of the wave trough, $\delta_s = 2.5$ mm and at the time of the wave crest, $\delta_s = 7$ mm (6–8 mm). In the same way, the sheet flow layer thickness under the crest and under the trough of the wave is determined for all the waves in wave group Gp, and for all the waves in wave group Gi (different flat bed sheet flow condition with $T_{gr} = 100$ s, $T_p = 6.4$ s, $H_s = 1.0$ m and a water depth above the sand bed of 3.0 m). In addition, values of sheet flow layer thickness have already been determined for six monochromatic wave conditions (see Dohmen-Janssen and Hanes, 2002). The values of the sheet flow layer thickness derived in this way are normalized by the mean grain size and plotted against the estimated Shields parameter θ in Fig. 10. For the measurements, the value of θ is calculated using a wave friction factor (that is, Swart, 1974) and a mobile-bed roughness height, according to the expression of Sumer et al. (1996), which is a function of the Shields parameter and the ratio of settling velocity to friction velocity. This figure also shows an expression for non-dimensional sheet flow layer thickness as a function of θ, derived by Sumer et al. (1996) for steady flow. We note that the true instantaneous bed shear stress is not well known, so the agreement shown in Fig. 10 may be fortuitous.

Fig. 9. Vertical concentration profile in the sheet flow layer under the crest and the trough of the highest wave in the wave group of condition Gp.
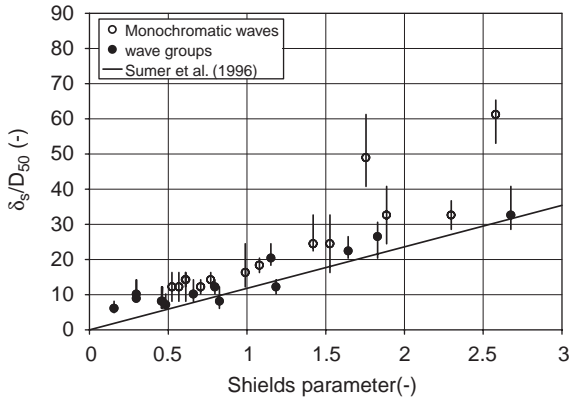
Fig. 10. Non-dimensional sheet flow layer thickness under crests and troughs of monochromatic waves and waves in two different wave groups against Shields parameter.

Fig. 10 shows that the sheet flow layer is of the order of 10 grain diameters thick. The measurements of non-dimensional sheet flow layer thickness seem to follow the linear relation with the estimated Shields parameter, as suggested by the expression of Sumer et al. (1996), although the sheet flow layer thickness under waves seems to be somewhat larger than in steady flow. Moreover, the values of sheet flow layer thickness under individual waves in a wave group are similar to those under monochromatic waves. This confirms the idea that the concentrations in the sheet flow layer are nearly instantaneously related to the near-bed hydrodynamics and do not depend significantly on the wave history.

3.4. Grain velocities

Grain velocities in the sheet flow layer were determined from a cross-correlation between the two concentration signals: the time-lag for which a peak in cross-correlation is observed (Δt) determines the horizontal grain velocity u_g, because the distance between the probes is fixed ($\Delta x = 15\,\mathrm{mm}$): $u_g = \Delta x / \Delta t$. Velocities were calculated at different elevations relative to the initial bed, as determined by the average elevation of each concentration bin. First, the concentrations signals were high-pass filtered. To determine the velocity within the wave group, each wave group was divided into 360

intervals. For each phase-interval of each wave group within a bin, the cross-correlation of the two concentration signals was determined. Next the cross-correlations of all the wave groups in a bin were averaged per phase-interval, in order to determine the ensemble-averaged cross correlation. For more details about the correlation technique, see McLean et al. (2001).

The upper panel of Fig. 11 shows the fluid velocities measured at 0.1 m above the bed, together with the grain velocities at different elevations in the sheet flow layer ($-0.9 - +2.1\,\mathrm{mm}$). Unfortunately, values of grain velocities could only be determined near the crest of the highest waves. Under the trough of the waves and under the smaller waves, velocities were apparently too small and/or the sheet flow layer was too thin to allow any significant cross-correlations to be detected. The figure shows that grain velocities very close to the bed are of the same order as the velocity outside the wave boundary layer. This can be seen even more clearly in the lower panel, which shows in detail the fluid and grain velocities under the highest wave in the group. As would be expected, grain velocities are largest at the highest elevation ($z = 2.1\,\mathrm{mm}$). However, even about 1 mm below the still bed level (which in this case is about 2–3 mm above the base of the sheet flow layer) grain velocities are still about 70% of the velocity outside the wave boundary layer. The lower panel also shows that grain velocities are ahead in phase compared to the velocity outside the wave boundary layer. This is also what would be expected in response to the fluid pressure gradient: due to the smaller inertia close to the bed the flow reversal and the maximum in velocity occur with a lead relative to the velocity away from the bed, similar to a clear fluid oscillatory boundary layer.

3.5. Sediment fluxes

As a result of the high concentrations close to the bed (see Figs. 4–8) and the relatively high grain velocities in this region (compared to the velocity outside the wave boundary layer, see Fig. 11), the instantaneous sediment fluxes inside the sheet flow layer are high. This can be seen in Fig. 12, which
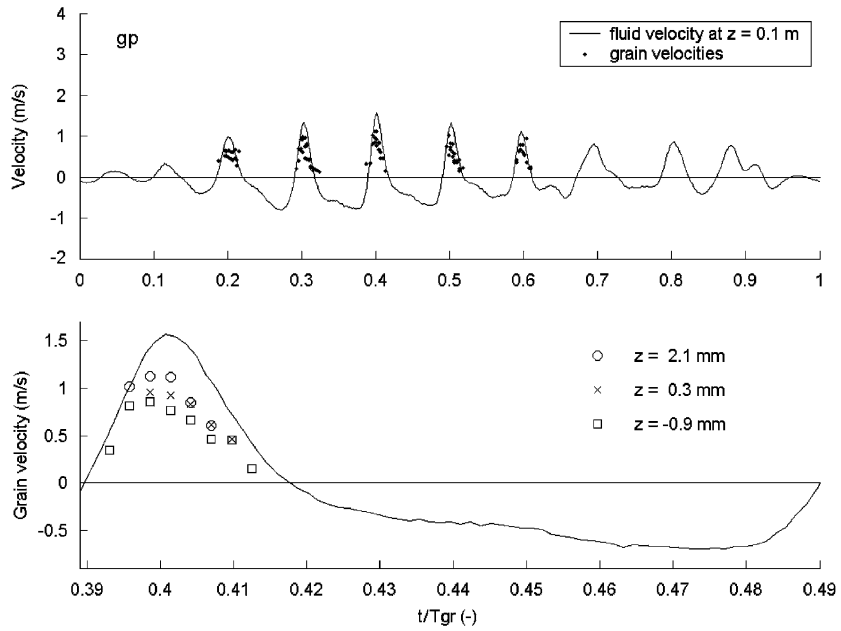
Fig. 11. Ensemble-averaged fluid velocities and grain velocities in the sheet flow layer. The upper panel shows all available measurements over the wave group. The lower panels shows in detail measurements under the highest wave in the group.
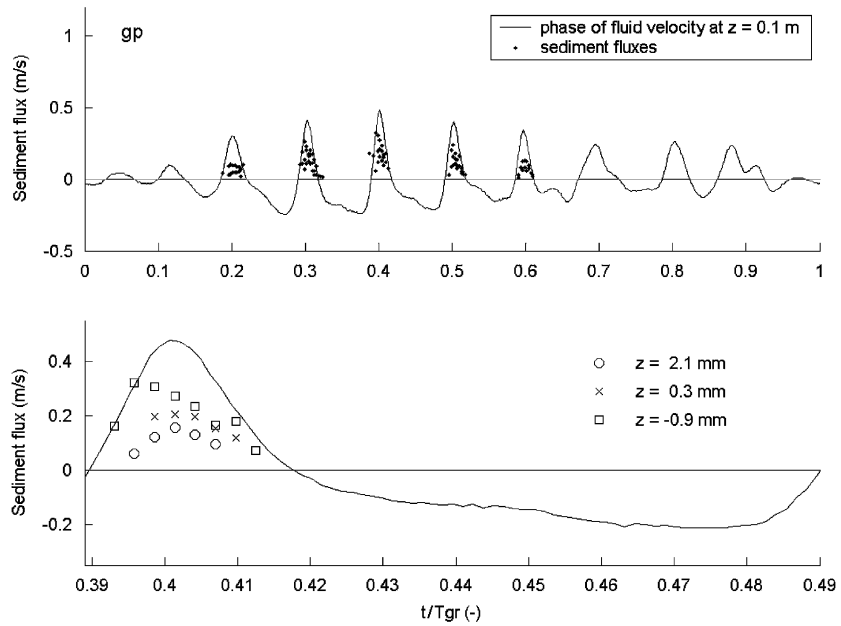

Fig. 12. Ensemble-averaged sediment fluxes in the sheet flow layer. The upper panel shows all available measurements over the wave group. The lower panels shows in detail measurements under the highest wave in the group.

shows the ensemble-averaged sediment fluxes in the sheet flow layer derived from the ensemble-averaged concentrations and ensemble-averaged grain velocities. Note that the flux is calculated as the concentration (in m^3/m^3) multiplied by the velocity (in m/s), giving units of sediment flux of m/s. (Integrating over the depth gives the transport rate in m^2/s (m^3/s per m width)). Ideally, it would have been more accurate to ensemble average the product of the velocity and concentration, but unfortunately this is not possible with present measurement techniques. The solid line in the figure is the fluid velocity at 0.1 m above the bed at an arbitrary scale and is just intended to show the phase in the wave group. Despite the fact that grain velocities are higher further away from the bed, sediment fluxes decrease with elevation, due to the strongly decreasing sediment concentrations.

Fig. 13 shows the vertical velocity profile (left-hand panel) and the vertical sediment flux profile (right-hand panel) under the crest of the highest

wave in the group. The open circles represent the measurements in the sheet flow layer (grain velocities and product of grain velocity and sheet flow concentration). The solid circle indicates the approximate level of the still bed (see Fig. 9), where the velocity—and thus the sediment flux—are expected to be zero. The dashed and solid lines represent two estimates of the fluid velocity profile and the suspended flux profile above the sheet flow layer. Inside the sheet flow layer, the estimated fluid velocity profiles are represented by the thin dotted lines.

The fluid velocity profiles are roughly estimated as a logarithmic profile with zero velocity at $k_s/30$ above the base of the sheet flow layer (with two different values of the roughness height k_s) and a value $u_{0.1}$ at the top of the wave boundary layer. Here, $u_{0.1}$ is the measured fluid velocity at 0.1 m above the bed, because the velocity is approximately constant above the wave boundary layer. The wave boundary layer thickness is estimated according to the expression of Sleath (1987) with a
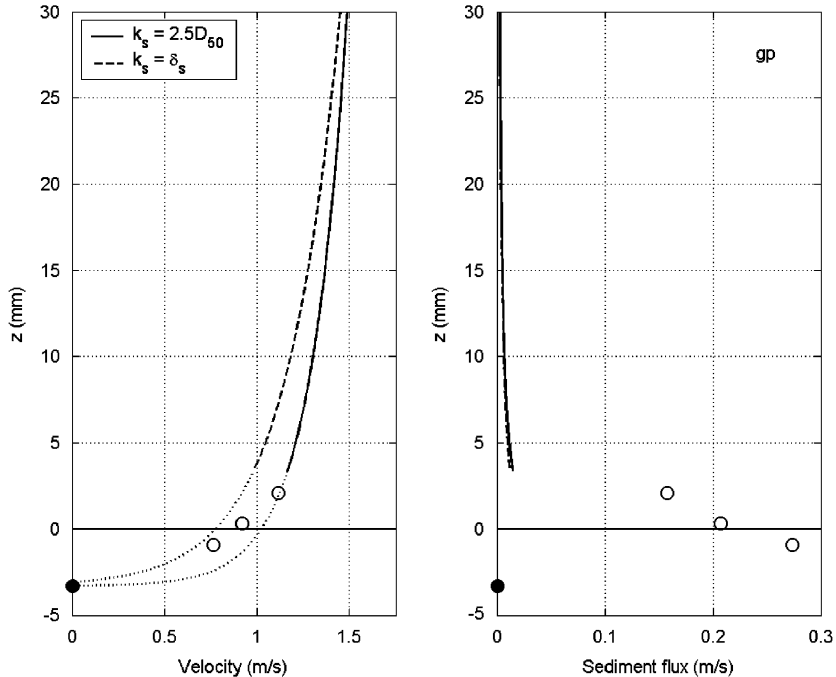

Fig. 13. Velocity and sediment flux profile under the crest of the highest wave. The open circles represent the measurements in the sheet flow layer. The solid circle indicates the approximate level of the still bed (zero velocity and zero sediment flux). The dashed lines represent an estimated fluid velocity profile and an estimated suspended flux profile.

roughness height of $2.5D_{50}$. The roughness height k_s, that determines the level where the velocity becomes zero, is assumed to be equal to $2.5D_{50}$ for the solid line and equal to the thickness of the sheet flow layer for the dashed line. A roughness height of $2.5D_{50}$ is usually assumed for a fixed plane bed. However, it is often suggested that under sheet flow conditions the thickness of the sheet flow layer, rather than the grain size, represents the roughness height (see, for example, Dohmen-Janssen et al., 2001; Dohmen-Janssen and Hanes, 2002). The sheet flow layer thickness is about 7 mm in this case (see Fig. 9 and accompanying text), or approximately 30 grain diameters.

The estimated suspended sediment flux profile is based on the estimated fluid velocity profile and a rough estimate of the suspended sediment concentrations under the crest of the highest wave. The latter are estimated as five times the value of the time-averaged suspended sediment concentrations in the lower 10 cm above the bed (measured by a pump sampling system), because Fig. 6 indicates that the maximum concentrations is—at most—about five times the time-averaged value.

Fig. 13 shows that high in the sheet flow layer the grain velocities are similar to the expected fluid velocity for a roughness height of $2.5D_{50}$. Lower in the sheet flow layer the grain velocities are smaller than this estimated fluid velocity, but seem to agree with fluid velocities estimated using an increased roughness height. The grain velocities closer to the stationary bed in the sheet flow layer are lower than the fluid velocities, due to the higher inertia of the grains compared to the fluid and due to collisions between the grains and other grain–grain interactions that take place between moving grains and the stationary bed. Unfortunately, it was not possible to obtain fluid velocities in this region to evaluate these hypotheses.

The right-hand panel of Fig. 13 shows that the sediment flux in the sheet flow layer is much larger than the suspended sediment flux. Again, it is emphasized here that a net current is absent in the flume. The presence of a net current (as is often the case in field conditions) is expected to lead to much higher suspended sediment fluxes. Fig. 13 also shows that the sediment flux continues to increase

towards the base of the sheet flow layer. As indicated by the level of the still bed, the sediment flux is expected to decrease to zero over a thin layer just above the base of the sheet flow layer. The fact that our measurements do not indicate a reduction in sediment flux near the stationary bed is a concern, and provides further motivation for additional experiments. It may be explained by the large velocity gradient in this region, where the velocity increases from zero at the base of the sheet flow layer to about 0.8 m/s, probably over less than a mm. We measured these grain velocities from a cross-correlation of two concentration signals. However, the height of the measuring volume of the concentration sensors is about 1–1.5 mm, which makes it impossible to measure grain velocities at different elevations within a mm.

3.6. Net sediment transport rates

To verify that the estimated magnitudes of the sediment flux are of the right order of magnitude, a rough estimate is made of the transport rate under the crest of the highest wave by integrating the flux profile from the bed to the highest measurement point. In the past, it has often been found that the sediment transport rate under sheet flow conditions is related to the third power of the velocity above the wave boundary layer. Therefore, the ratio between the transport rate under the crest of the highest wave ($q_{s,chw}$) and the third power of the velocity under the crest of the highest wave (u_{chw}) is determined by

$$A = \frac{q_{s,chw}}{u_{chw}^3}.$$

This ratio, together with the third power of the ensemble-averaged time series of the velocity during the highest wave in the group ($u_{hw}^3(t)$), is used to calculate the transport rate during the highest wave in the group ($q_{s,hw}(t)$):

$$q_{s,hw}(t) = A^* u_{hw}^3(t).$$

Next, this value is integrated over the wave period of the highest wave in the group to find an estimate of the *net* transport rate for the highest wave in the group $\langle q_{s,hw} \rangle$. This value is plotted against the value of the third power velocity moment in
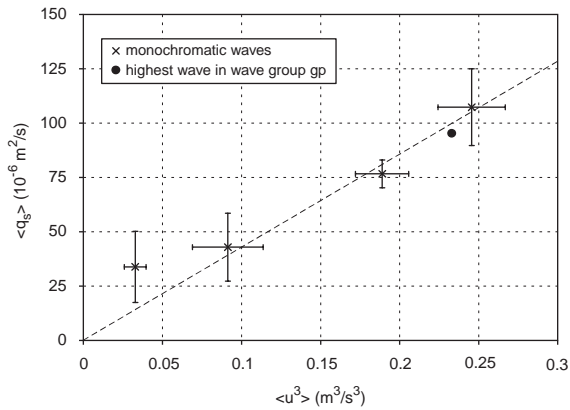
Fig. 14. Net sediment transport rate for monochromatic waves and for the highest wave in wave group Gp as a function of the third power velocity moment.

Fig. 14. This figure also includes results from the monochromatic wave experiments (see Dohmen-Janssen and Hanes, 2002). In those experiments, net transport rates were determined from the change in bed level before and after each run. This technique cannot be used to give an additional estimate of the net transport rate under the highest wave in the group, because the change in bed level will be determined by all the waves in the group. Fig. 14 shows that the net transport rate under the highest wave in the group (estimated from the flux profile under the crest of the highest wave) falls on the same line as the net transport rates under monochromatic waves (measured using the mass conservation technique). This is a promising result, which indicates that the sediment flux values shown in Figs. 12 and 13 are realistic. Moreover, because the transport is concentrated in the sheet flow layer, this confirms the earlier observations that sheet flow processes are determined by the individual waves, rather than by the history of the wave group. It remains as future work to more completely examine the flux relationship over the entire period of the wave group.

4. Conclusions

Measurements of sediment concentrations in the sheet flow layer and in the suspension layer, as well as of grain velocities and sediment fluxes in the sheet flow layer have been presented. The measurements were carried out under prototype waves in the Large Wave Flume in Hannover, Germany. This paper focuses on the tests with repetitive wave groups in the flat bed sheet flow regime.

The following conclusions can be drawn from the measurements:

- Concentrations in the sheet flow layer are highly coherent with the instantaneous near-bed hydrodynamics: concentrations show (relatively sharp) peak values under the crests of the waves and these peak values increase for increasing wave heights (increasing crest velocities). When the waves decrease again (further into the wave group), the peak values of the concentration decrease too.
- Concentrations in the suspension layer respond much more slowly to changes in near-bed velocity: the decrease in concentration during flow deceleration occurs much slower than in the sheet flow layer. Further away from the bed, the concentration continues to increase when the waves start to decrease again: the concentrations increase and decrease over the time scale of the wave group, with a time delay relative to the peak wave within the wave group.
- The thickness of the sheet flow layer under a particular wave is related to the velocity under that wave and does not depend on the preceding wave. This confirms the observed nearly instantaneous behaviour of the concentrations in the sheet flow layer. The absence of a time lag between velocity and concentration (in contradiction to simulations recently presented by Hsu and Hanes, 2004) might be attributed to the fact that the peak acceleration occurs very close in time to the peak velocity for the highly non-linear waves in these experiments.
- The non-dimensional sheet flow layer thickness (normalized by the grain diameter) under the crest and the trough of the wave is linearly related to the estimated Shields parameter and agrees reasonably well with the expression of Sumer et al. (1996) that was derived for steady flow.

- Grain velocities inside the sheet flow layer have values that are similar to (or slightly smaller than) expected fluid velocities. The smaller velocities low in the sheet flow layer, compared to the fluid velocities that would be expected above a fixed plane bed may be explained by the inertia of the grains and/or the interactions between the moving grains and the stationary bed.
- Instantaneous sediment fluxes inside the sheet flow layer are at least an order of magnitude bigger than in the suspension layer for these conditions without a net current. Integration of the sediment flux profile over depth and wave period yields similar values for the net transport rate as for monochromatic waves.

References

Bagnold, R.A., 1956. The flow of cohesionless grains in fluid. Philosophical Transactions of the Royal Society of London (A) 249 (964), 235–297.

Dibajnia, M., Watanabe, A., 1992. Sheet flow under non-linear waves and currents. Proceedings of the 23rd International Conference on Coastal Engineering. Venice, pp. 2015–2028.

Dohmen-Janssen, C.M., Hanes, D.M., 2002. Sheet flow dynamics under monochromatic nonbreaking waves. Journal of Geophysical Research 107 (C10) 10.1029/2001JC001045.

Dohmen-Janssen, C.M., Hassan, W.N., Ribberink, J.S., 2001. Mobile-bed effects in oscillatory sheet flow. Journal of Geophysical Research 106 (C11), 27,103–27,115.

Dohmen-Janssen, C.M., Kroekenstoel, D.F., Hassan, W.N., Ribberink, J.S., 2002. Phase-lags in oscillatory sheet flow: experiments and bed load modelling. Coastal Engineering 46 (1), 61–87.

Hanes, D.M., 1991. Suspension of sand due to wave groups. Journal of Geophysical Research 96 (C5), 8911–8915.

Hay, A.E., Bowen, A.J., 1994. On the Coherence Scales of Wave-Induced Suspended Sand Concentration Fluctuations. Journal of Geophysical Research 99, 12,749–12,765.

Hsu, T.J., Hanes, D.M., 2004. The effects of wave shape on sheet flow sediment transport. Journal of Geophysical Research 109 (C5).

King, D.B., 1991. Studies in oscillatory flow bedload sediment transport. Ph.D. Thesis, University of California, San Diego.

McLean, S.R., Ribberink, J.S., Dohmen-Janssen, C.M., Hassan, W.N., 2001. Sand transport in oscillatory sheet flow with mean current. Journal of Waterway, Port, Coastal and Ocean Engineering ASCE 127 (3), 141–151.

Ribberink, J.S., Al-Salem, A.A., 1994. Sediment transport in oscillatory boundary layers in cases of rippled bed and sheet-flow. Journal of Geophysical Research 99 (C6), 12,707–12,727.

Ribberink, J.S., Al-Salem, A.A., 1995. Sheet flow and suspension in oscillatory boundary layers. Coastal Engineering 25, 205–225.

Ribberink, J.S., Dohmen-Janssen, C.M., Hanes, D.M., McLean, S.R., Vincent, C.E., 2000. Near-bed sand transport mechanisms under waves: a large-scale flume experiment (SISTEX99). Proceedings of the. 27th International Conference on Coastal Engineering, July 2000, Sydney.

Sleath, J.F.A., 1987. Turbulent oscillatory flow over rough beds. Journal of Fluid Mechanics 182, 369–409.

Sumer, B.M., Kozakiewicz, A., Fredsoe, J., Deigaard, R., 1996. Velocity and concentration profiles in sheet-flow layer of movable bed. Journal of Hydrologic Engineering ASCE 122 (10), 549–558.

Swart, D.H., 1974. Offshore sediment transport and equilibrium beach profiles. Delft Hydraulics Laboratory, Publication No. 131, Delft Hydraulics, The Netherlands.

Thorne, P.D., Hanes, D.M., 2002. A review of acoustic methods for the study of small scale sediment transport processes. Continental Shelf Research 22, 603–632.

Vincent, C.E., Hanes, D.M., 2002. The accumulation and decay of nearbed suspended sand concentration due to waves and wave groups. Continental Shelf Research 22/14, 1987–2000.